Experimental validation of the screw compressor oil drag model for various rotor profiles

Suraj Abdan[1,2*], Sumit Patil[1,2], Nikola Stosic[1], Ahmed Kovacevic[1] and Ian Smith[1]

[1] Centre for Compressor Technology, City, University of London, London, U.K.
[2] Kirloskar Pneumatic Company Limited, Pune, India.

E-mail: suraj.abdan@kirloskar.com, sumit.patil@kirloskar.com, n.stosic@city.ac.uk, a.kovacevic@city.ac.uk, i.k.smith@city.ac.uk

*Corresponding author

Abstract: Injecting oil inside the compressor chambers of the oil-flooded, twin-screw compressors has several advantages. Oil cools the compressing fluid upon mixing with it and hence the compression process is brought nearer to the ideal isothermal compression process. The oil also serves as a lubricant between the meshing rotors and other clearance gaps in the compressor. The thin film of oil formed in the clearance gaps prevents internal leakages too; enhancing the volumetric efficiency of the compressor. Among these desirable effects of injecting oil in screw compressors, there is an undesirable effect too. The interaction (friction) of oil films formed in various clearance gaps with the rotors leads to a drag power loss. Recent studies such as Abdan et. al (2022) have proposed more detailed and accurate methods to estimate the oil drag losses in screw compressors. These methods enable the modelling of the effect of even minor changes in rotor profile on the drag loss power. Predictions of this model were hence used to tweak the screw rotor profiles with an objective to reduce the oil drag losses. Such profiles were then retrofitted in the existing machines and tested. Comparing the differences in power consumption of these machines, the component of oil drag loss was deduced. The experimental results show close agreement with the oil drag loss prediction model. The reduction of oil drag losses through profile modifications led to an improvement of the specific power of oil flooded screw compressor.

Keywords: Energy efficiency, Oil drag, Radial clearance, Axial clearance, Interlobe clearance, Screw Compressor

Nomenclature

Symbol	Description	Unit
A	shear area	m^2
h	total/radial clearance gap	m
N	rotational speed	rpm

p	pressure	Pa
r	radius	m
P	power	W
P_{ad}	adiabatic power of compression	W
T	torque	Nm
u, v and w	velocity	m/s
V	tip speed	m/s
g	acceleration due to gravity (9.8 m/s^2)	m/s^2
x, y and z	spatial coordinates	
p_1	suction pressure	Pa
p_2	discharge pressure	Pa
V_1	suction volume flow	m^3
n	adiabatic index	
Greek symbols		
ρ	density	kg/m^3
μ	dynamic viscosity	Ns/m^2
π	pressure ratio	
τ	shear stress	N/m^2

1. Introduction

The use of twin-screw compressors is gaining popularity because of their higher efficiency and better reliability than reciprocating and turbo counterparts for medium flow rates and power inputs. In an oil-flooded screw compressor, the injection of oil during the compression process helps in achieving near isothermal compression. Along with the cooling of the compressed gas, the injection of oil lubricates the rotating parts of the compressor and also seals the clearance gaps. However, the undesirable effect of the circulation of oil is an increase in the consumption of power where the shearing of oil in the clearance gaps induces drag loss. Therefore injecting the optimum amount of oil is very important to achieve the best performance from the oil injected screw compressor. Accurate predictions of the oil drag losses can help design optimal oil injection quantities.

Numerous mathematical models and commercial programmes are available for the prediction of the mechanical efficiency of the screw compressor. Although the prediction from these methods matches well with the experimental measurements, the identification of elements of the compressor contributing to power loss and quantification of their contribution to total power loss is not reported in

these methods. A study by Abdan et al. (2018) presented that the elements that contribute to mechanical power loss are the anti-friction bearings, drag loss caused by shearing of oil, shaft seal and power loss in drive systems like the gear or belt drive mechanism, if present. It is shown that the anti-friction and oil drag loss are the major contributors to mechanical power loss in the screw compressor. The literature published by SKF, and Harris and Kotzalas (2006) reports the prediction of anti-friction bearing power loss using empirical correlations. These methods quantify the power loss from the bearings into load-dependent and load-independent losses. The experimental validation of these methods is reported by Tu (2016). From the comparison of experimental measurements and predictions from the methods for cylindrical roller bearing which takes the radial load, it is concluded that the Harris model predictions fit well as compared to other two models. Similar analysis and comparison is presented for angular contact ball bearings by Gradu (2000) where it is shown that the Harris model predictions capture the changes in load and speed better than the other two models. However, the prediction and experimental validation for oil drag loss within the screw compressor has not been much reported. Deipenwisch and Kauder (1999) presented that the excess amount of oil can lead to substantial and undesirable change in the performance of the screw compressor. The results of a comparison between an analytical model and computational fluid dynamics (CFD) simulation for the prediction of oil drag loss in the radial and axial clearances of the screw expander and compressor are reported by Gräßer et al. (2014). In addition, Gräßer et al. (2015) presented a study that compared the advantage of sealing the clearances, with the disadvantage of the resulting increased frictional loss. Gräßer et al. (2016) compared the performance of liquid-flooded and dry expanders at different operating speeds and the effect of varying the viscosity of the injected liquid on the performance of a liquid-flooded screw expander. Assuming the flow paths of the injected oil are rectangular in cross section, a 2 dimensional multiphase CFD study was published by Vasuthevan et al. (2018), which showed how the hydraulic loss is affected both by the amount of oil injected and the rotational speed of the rotors. It showed that increases in both these effects increase the loss.

From the works of literature studied, it is understood that although enough computational studies are available, the comprehensive analytical models published for the prediction of oil drag loss are limited. Also, the lack of experimental validation of the analytical models was seen in the literature. The study presented here is a part of an extension to the previous study which was published by Abdan et. al. (2022) on formulating an analytical model for the prediction of oil drag loss within an oil-flooded, twin-screw compressor. In that study, three clearance gaps are identified where the shearing of oil takes place and they are; radial clearance, interlobe clearance and axial clearance. The radial clearance is formed between the outer diameter of the rotors and the housing bore diameter in which rotors rotate while the interlobe clearance is formed between the lobes of two meshing rotors. The high-pressure discharge side of the compressor maintains the axial clearance between the rotor side end faces and the housing. Figure 1 represents different clearances that are present inside the twin-screw compressor through which the oil shears.

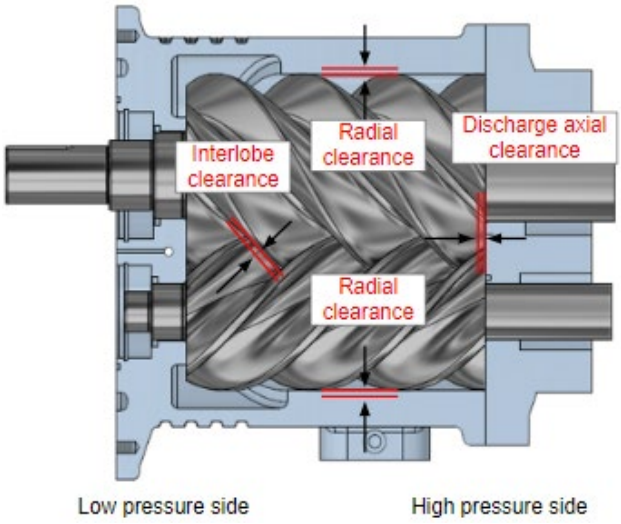

Figure 1: Different clearances within the screw compressor

As oil in clearance gaps experiences inertial as well as a pressure-induced flow, a superimposed Couette-Poiseuille flow model with planar representation is used to calculate the oil drag in the above-mentioned clearances. A parametric analysis is presented in Abdan et. al. (2022) to understand the effect of pressure ratio and tip speed for different sizes of the compressors. It indicates that from total drag loss, the loss in the axial clearance is nearly 2/3rd of the total drag loss while that in the radial clearance is 1/3rd of the total drag loss. However, relatively negligible loss is caused in the interlobe clearance between the rotors for all sizes of the compressor. The parametric analysis for the change in pressure ratio showed that the axial and radial clearance drag losses show negligible change with respect to pressure ratio while the interlobe clearance drag loss shows a considerable change. As the viscosity of oil increases, the increase in oil drag loss is more pronounced in the bigger size of the compressors as compared to the smaller sizes. The magnitude of change of the clearances also affects the drag loss where the change in the magnitude of axial and radial clearances has a considerable effect on the drag loss whereas the change in magnitude of the internal clearance does not affect the drag loss much. Although the paper presents an analytical model and comprehensive parametric analysis, the lack of experimental investigation and validation motivated authors to extend this study further.

This study is extended for experimental validation of the analytical model for drag loss by designing and manufacturing three different screw rotor profiles. These screw rotor profiles were designed in such a way that each rotor profile demonstrates characteristics of either anticipated increase or decrease in drag loss. The performances, mainly the shaft power of these screw rotor profiles, were experimentally measured by assembling them, one after the other, in the same compressor housing and operating it at the same operating conditions. An air screw compressor package of 55 kW electric motor frame size was used to perform the experiments. The rotors had particularly high tip speed (~40m/s) in order to pronounce the effect of drag in the experimental setup. The volumetric flow rate normalised at suction conditions and package input power were measured during the experiments. From the package input power, the shaft power of the bare screw compressor is back-calculated by deducting the auxiliary powers like cooler fan motor power, control panel power and main drive

motor efficiency. Finally, the shaft power predictions for three different screw rotor profiles were compared with the experimental measured shaft powers to validate the analytical model proposed in the previous paper of this series.

2. Drag loss prediction model to predict the influence of screw rotor profile on total drag

The optimum level of oil injection in a screw compressor is an important parameter to be defined. Although injection of oil serves three purposes; for the cooling, the lubrication and the sealing of the clearance gaps, the excess amount of oil not only increase the drag loss, it also increases the cooling load on the oil cooler of the screw compressor package. Therefore to evaluate the optimum quantity of oil injection level, a simple analytical model was developed that can predict the drag loss caused in different clearance gaps. This analytical model is based on the superimposed Couette-Poiseuille flow model as the oil in clearance gaps experiences inertial as well as the pressure-induced flow. The velocity profile generated, in the radial clearance between the tip of the rotor and the bore of the housing, because of the opposing effects of pressure-induced and inertial flow is shown in Figure 2.

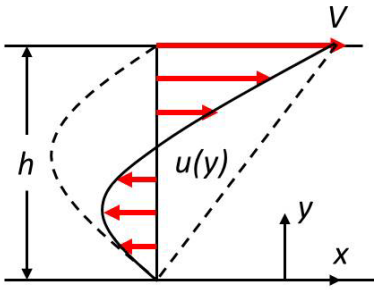

Figure 2: Couette-Poiseuille velocity profile

The top plate indicates the rotor tip velocity, V, while the bottom plate represents the stationary housing boundary. These two are separated by the clearance height, h. The dotted velocity profile lines on the right side indicate pure Couette flow while that on the left side indicates only Poiseuille flow. The resultant velocity profile takes the form as presented by the continuous line, u(y). The assumptions made during the development of the model are as follows:

- The planar representation of Couette-Poiseuille flow is considered
- The pressure gradient remains constant across all clearance gaps
- The flow is steady with the clearance gaps completely filled with oil
- The fluid is incompressible and Newtonian with constant properties
- There is no flow in the y and z direction

Using the conservation laws for mass which reduces to a single term

$$\frac{\partial u}{\partial x}+\frac{\partial v}{\partial y}+\frac{\partial w}{\partial z}=0 \qquad \frac{\partial u}{\partial x}=0 \tag{1}$$

and momentum equation

$$\rho\left[\frac{\partial u}{\partial t}+u\frac{\partial u}{\partial x}+v\frac{\partial u}{\partial y}+w\frac{\partial u}{\partial z}\right]=-\frac{\partial p}{\partial x}+\rho g_x+\mu\left[\frac{\partial^2 u}{\partial x^2}+\frac{\partial^2 u}{\partial y^2}+\frac{\partial^2 u}{\partial z^2}\right] \tag{2}$$

with boundary conditions at the rotor tip and housing inner surfaces, it reduces to the velocity profile

$$u = \frac{Vy}{h} + \frac{1}{2\mu}\frac{\partial p}{\partial x}(y^2 - hy) \tag{3}$$

After substituting this velocity profile in the shear stress equation, the shear stress can be calculated as

$$\tau = \mu\frac{\partial u}{\partial y} \qquad \tau = \frac{\mu V}{h} + \frac{h}{2}\frac{dp}{dx} \tag{4}$$

Ultimately, the torque required overcoming the shear stress and power loss is given by

$$T = \tau A r \qquad P = \frac{2\pi N T}{60} \tag{5}$$

As the clearance gaps are in micrometre magnitude, the first term in Eq. (4) which represents Couette flow becomes dominant over the second term which is Poiseuille flow and this reasonably supports the assumption of a constant pressure gradient.

For the calculation of shear area in the radial clearance, the top land width of the rotors times the lead and number of lobes is taken for the calculation. In the case of interlobe clearance, the sealing line length times the top land width across the flow is considered for the shear area calculation. Although the velocity boundary changes in the radial direction, the tip velocity at pitch circle radius and circular area at pitch circle of the rotor is considered for the calculation of shear stress and frictional torque. The drag areas for radial, axial and interlobe clearances are shown in Figure 3.

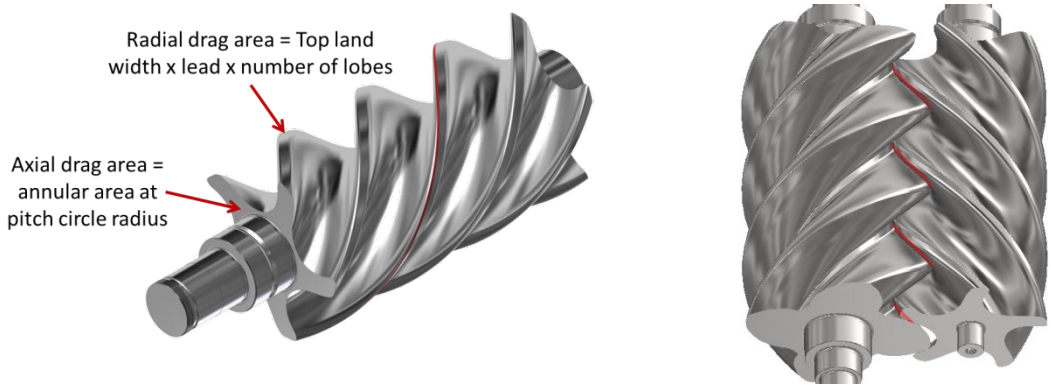

(a) Radial and axial drag area (b) Interlobe drag area

Figure 3: Representation of drag areas

To experimentally validate the developed analytical model for oil drag loss, it can be understood that only changes in the shear area on the rotor profiles could substantially influence the drag loss. As presented in the previous paper of this series, the drag loss in interlobe clearance does not contribute much to the power loss. Also, the changes in the shear area of axial clearance could demand substantial changes in the manufacturing and a possibility of affecting the other performance parameters. So it was decided to make changes only in the shear area of the radial clearance while designing different screw rotor profiles.

3. Rotor profiles designed for different levels of drag losses

A patented 'N' rotor profile (Stosic, 1997); designed by City, University of London researchers was taken as a reference profile. Based on this profile, two modified screw rotor profiles, 'Beta-1' and 'Beta-2', were designed by the Kirloskar team. The characteristic of the 'Beta-1' profile is that it has a slanting gate rotor top-land. It can be generated easily with any N-profile either by use of variable tip clearance or through tweaking the curve that generates this portion of profile. The slanting is provided from the leading edge of the profile to the trailing edge such that the minimum radial clearance is only along a fine line following the rotor casing (Figure 4). With this change, it is anticipated that the shearing of the oil in the radial clearance will reduce and ultimately the drag loss. The 'Beta-2' profile is provided with a longer top-land width than the 'N' screw rotor profile and is expected to contribute higher drag loss. The schematic representation of 'N', 'Beta-1' and 'Beta-2' gate rotor top lands is shown in Figure 6. The red marked portion on top of each gate rotor depicts the area of minimum radial clearance where oil film shears.

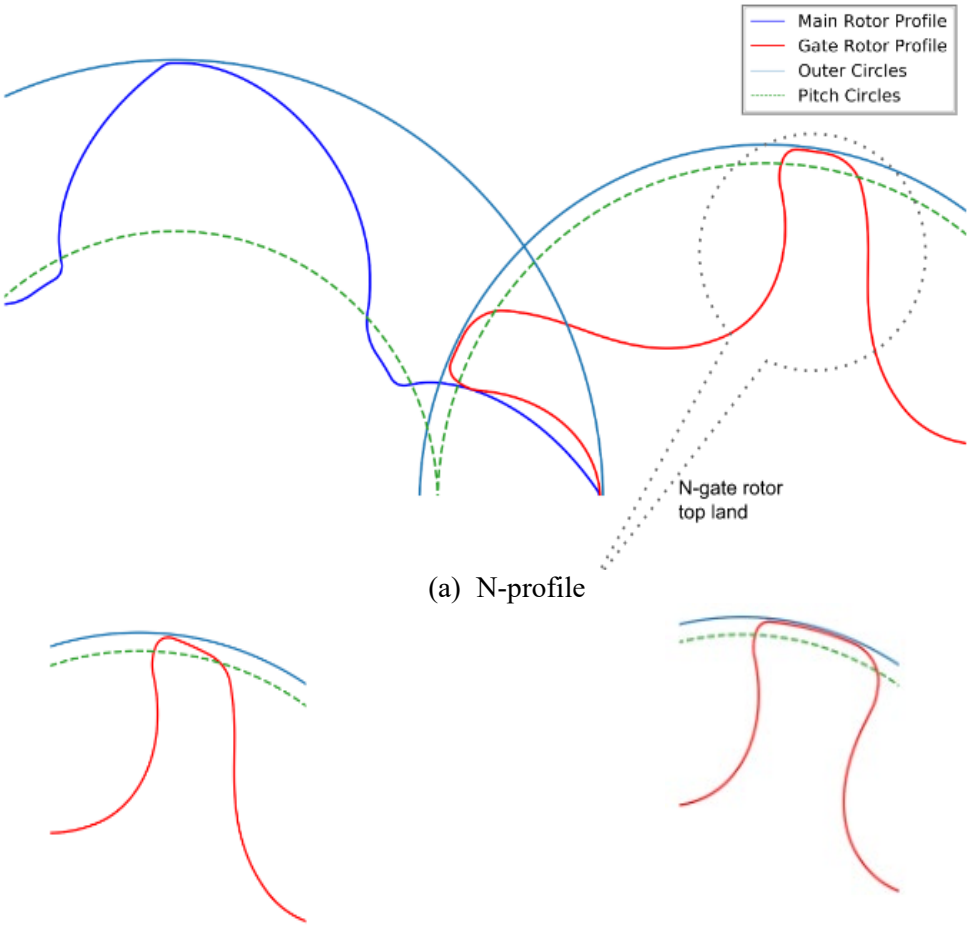

(a) N-profile

(b) Beta-1 profile

(c) Beta-2 profile

Figure 4: Schematic representation of slanting gate rotor top land in Beta-1 profile and Beta-2 profile compared to the flat land on N-profile

The changes in 'Beta-1' and 'Beta-2' profiles over 'N' profile were implemented on the rack profiles using principle of rack generation (Hanjalic & Stosic 1997) to generate respective profiles. The 'N'

profile rack was modified towards its ends to incline by few degrees to create a slanting effect on gate rotor top land. Figure 5 (a) represents the 'Beta-1' rack profile superimposed over the 'N' rack. To generate 'Beta-2' profile, N rack had to be modified in more ways than 'Beta-1'. The low pressure side of rack has to be flattened to increase the thickness of gate rotor lobes. The rack ends need to be longer too in order for the top land to be wider. Figure 5 (b) represents the 'Beta-2' rack profile superimposed over the 'N' rack.

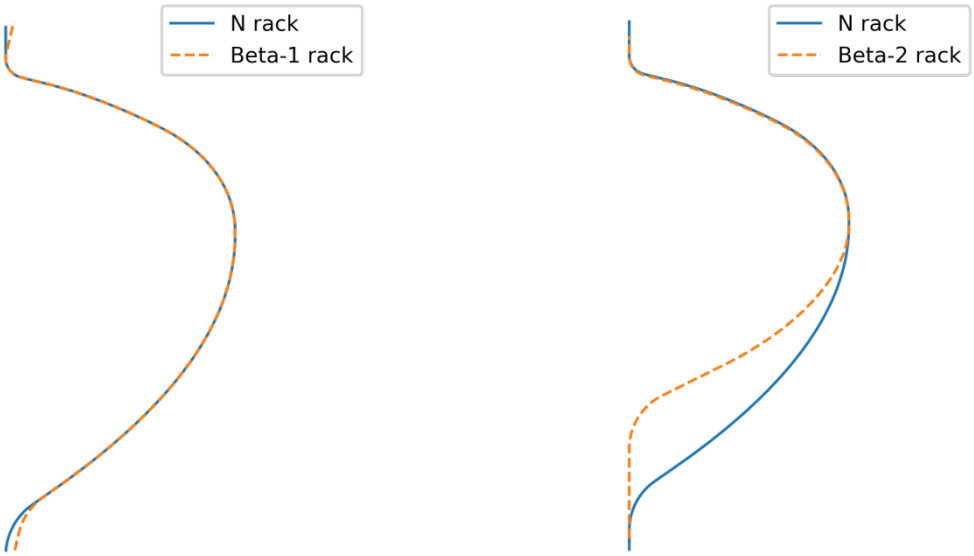

(a) Rack profiles of N and Beta-1 (b) Rack profiles of N and Beta-2

Figure 5: Rack profiles of N, Beta-1 and Beta-2

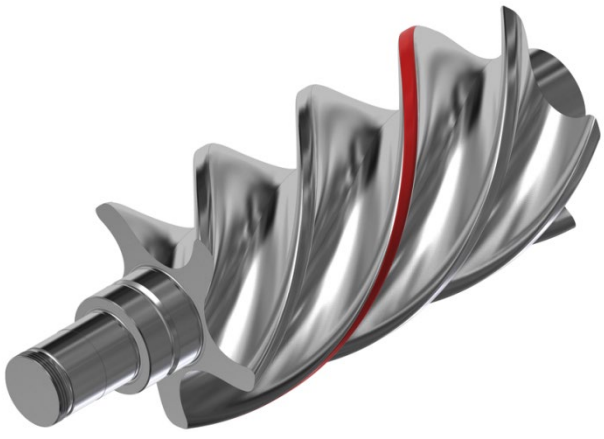

(a) N-profile

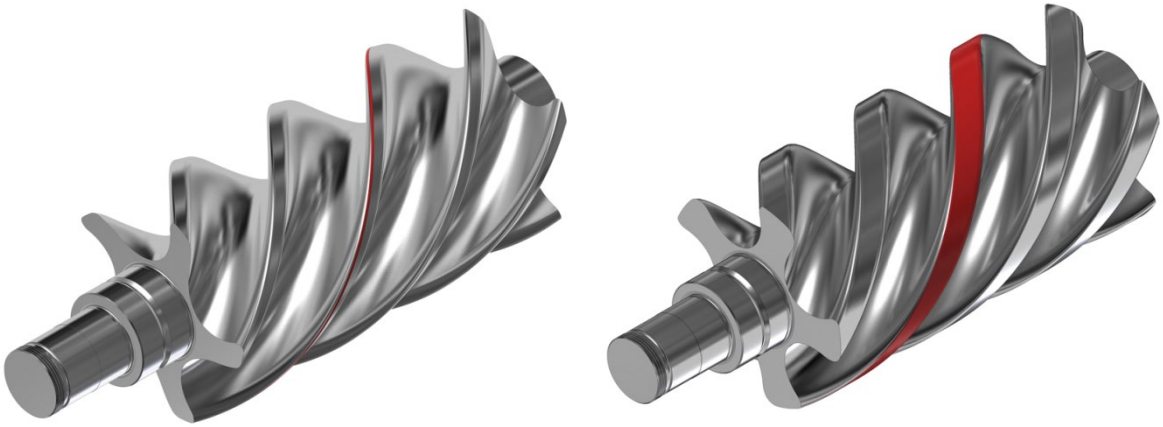

(b) Beta-1 profile (c) Beta-2 profile

Figure 6: Schematic representation of 'N', 'Beta-1' and 'Beta-2' gate rotor top lands where oil film shears in the radial gap leading to drag losses

As indicated by Abdan et al. (2021) with the increase in tip speed, the contribution of the oil drag loss increases and can be more than that of the bearing power loss. So the experiments were carried out at relatively higher tip speeds to amplify the effects caused by the oil drag losses.

4. Experimental measurements

An oil-flooded, twin-screw, air compressor packaged unit with a drive electric motor of 55 x 1.2 kW rating was used for the experimentation. This is shown in Figure 7. Due to confidentiality reasons, the size of the bare screw compressor could not be presented here. The lobe combination of the main and gate rotor used is 4/5 which was driven through a speed increasing gear ratio by an electric motor.

Figure 7: A Kirloskar 55 kW oil-flooded, twin-screw, air compressor package

The profile geometric characteristics of different rotor profiles and maintained assembly clearances are mentioned in the following Table 1.

Table 1: Profile geometric characteristics and assembly clearances

	N	Beta-1	Beta-2
GAPI [mm]	0.040	0.040	0.040
GAPA [mm]	0.060	0.060	0.060
GAPR [mm]	0.040	0.040	0.040
Interlobe leakage area [mm^2]	24.476	24.154	27.510
Gate rotor top land width [mm]	14.0	14.0	24.0

Here, GAPI stands for interlobe clearance, GAPA stands for axial clearance on high-pressure side of the compressor and GAPR stands for radial clearance. The interlobe clearance between rotors acts as a leakage path. It is similar for N and Beta-1 due to only small difference in these two profiles. Beta-2 has wider gate rotor lobes which increase this interlobe leakage area. This difference in leakage area affects the internal leakages and hence the flow and power of the machine. This effect is well captured by the chamber model calculations used for predicting flow and power for each case.

The rotors were manufactured in-house on precision grinding machines with a profile accuracy of 7 micrometres. The variation of profile all across the rotors by 7 micrometres may lead to up to 2% variation in measurable such as flow and power due to its effect on leakage areas. In real rotors, the variation is non-uniform across the profile as well as rotor lengths and hence the profile form deviation will only introduce an uncertainty of the order <1%. Figure 8 shows the actual photographs of manufactured rotors with above mentioned rotor profiles.

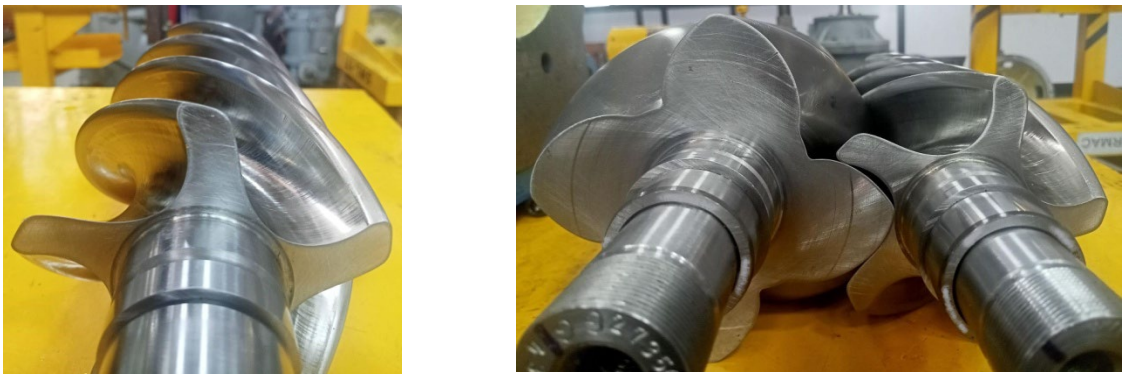

(a) Beta-1 profile

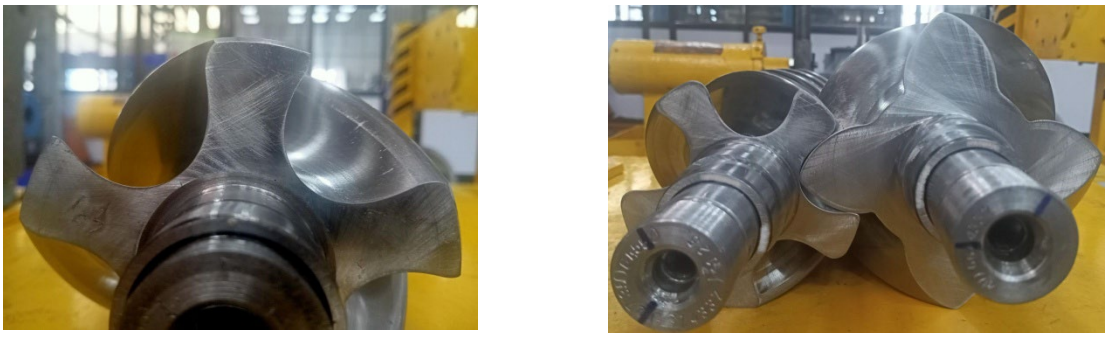

(b) Beta-2 profile

Figure 8: Actual photographs of rotors with the tweaked profiles ‘Beta-1’ and ‘Beta-2’

These rotors were assembled in the same bare compressor housing, one after the other, and were operated at a package discharge pressure of 7 bar (g). The compressor was driven by an electric motor through a gearbox with the main rotor rotating at a constant tip speed of 37.3 m/s. A single point oil-injection was provided in the bare compressor housing from the gate rotor side. The oil with density of 860 kg/m3 and operating viscosity of around 9 cSt was used. The volume flow rate was measured using a differential manometer at the discharge end of the compressor package and was normalised at the suction conditions.

5. Results and discussion

The experimental measurement of shaft power is a combined measurement of adiabatic power and total mechanical power loss. The total mechanical power loss includes losses arising from oil drag, the bearings, shaft seal and the gears. Since the same compressor with the same set of bearings, shaft seal and gears was used and operated at the same operating condition during the experiments, the power loss from the bearings, shaft seal and gears was considered constant. This is justified because operating conditions affecting loads remain constant. The prediction for bearing power loss is calculated using Harris model while the shaft seal power loss is predicted using a combined method proposed by Abdan et al. (2021). From the predictions, the power loss from the bearings calculated is 5.74 kW and that from the shaft seal is 0.05 kW. An assumption of 2% power loss in gears is considered in all cases for the calculation of total shaft power.

Using the superimposed Couette-Poiseuille method presented in above section for the calculation of drag loss, the results for drag loss at different clearances for ‘N’, ‘Beta-1’ and ‘Beta-2’ is shown in Table 2.

Table 2: Drag loss prediction for ‘N’, ‘Beta-1’ and ‘Beta-2’

	Power loss [kW]	**‘N’**	**‘Beta-1’**	**‘Beta-2’**
2a	**Bearing + seal**	**5.79**	**5.79**	**5.79**
2b	Drag loss in radial clearance	1.59	0.80	2.61

2c	Drag loss in high pressure axial clearance	1.82	1.82	1.82
2d	Drag loss in interlobe clearance	0.05	0.05	0.10
2e	**Total drag loss (2b+2c+2d)**	**3.46**	**2.67**	**4.53**
	Change in drag loss with respect to 'N'	-	-22.83%	30.92%

The change in drag loss between for 'Beta-1' and 'Beta-2' with respect to 'N' are presented in the last row of the Table 2. A substantial reduction in drag loss for 'Beta-1' while increase in it for 'Beta-2' is predicted by the method proposed in the previous section.

The results obtained for the experimental measurement of suction volume flow rate (FAD) and the compressor shaft power is indicated in Table 3.

Table 3: Experimental measurements for 'N', 'Beta-1' and 'Beta-2'

	Experimental measurements	**'N'**	**'Beta-1'**	**'Beta-2'**
3a	Compressor flow rate [m^3/min]	8.75	8.82	9.10
	% change with respect to 'N'	-	0.87%	4.0%
3b	Compressor shaft power measured [kW]	55.33	54.89	61.52
3c	Volumetric efficiency [%]	85.11	85.81	84.54
3d	Adiabatic efficiency [%]	74.99	76.25	70.15
3d	Indicated efficiency [%]	90.05	90.14	84.28

Mechanical loss is obtained as adifference between the shaft power and indicator power calculated by numerical simulation model, SCORPATH (Screw Compressor Optimal Rotor Profiling And THermodynamics) developed by (Stosic, 2005) for the measured flow rate. Oil drag is calculated as a difference between these mechanical losses and the gear, bearing and seal losses which are fairly constant for all three rotors in question.

As usual, the volumetric efficiency is a ratio between the compressor flow and its theoretical flow, adiabatic efficiency is a ratio between the compressor shaft power and the compressor isentropic power, while indicated efficiency is ratio between the compressor indicator power and its isentropic power. All of them, the volumetric, adiabatic and indicated efficiency show superiority of the 'Beta-1' over the 'Beta-2' and 'N' profiles.

Table 4 indicates the drag loss post-processed from the experimental measurement of the total shaft power.

Table 4: Post-processed drag loss from experimental measurements

	Experimental measurements	**'N'**	**'Beta-1'**	**'Beta-2'**
4a	Adiabatic power [kW]	41.59	41.95	43.26
4b	Power loss [kW]: Gear +bearing +seal	6.90	6.89	7.02
4c	Drag loss [kW] (3b-4a-4b)	6.84	6.05	11.24
	Drag loss change with respect to 'N'		-11.6%	64.3%

From the comparison presented in the Table 2 and Table 4 for drag loss prediction and post-processed values from experimental measurement, it is seen that trend for drag loss reduction in 'Beta-1' and increase in 'Beta-2' is in line with experimental observation. However, the prediction for percentage change in absolute values is not very well matching with the changes recorded in the experimental measurements. This can be due to the difference in prediction and actual power loss for other components like bearings, seal and gear. Alternatively, if the shaft power is predicted by using addition of adiabatic power and power loss from gear, drag loss, bearings and seal, the percentage difference between shaft power matches very well matches the experimental measurements as indicated in Table 5.

Table 5: A comparison of prediction and measured shaft power 'N', 'Beta-1' and 'Beta-2'

	Normalised parameters	**'N'**	**'Beta-1'**	**'Beta-2'**
(A)	Corrected prediction of shaft power	52.50	52.08	58.23
	% change with respect to 'N'	-	-0.80%	9.84%
(B)	Compressor shaft power measured [kW]	55.33	54.89	61.52
	% change with respect to 'N'	-	-0.80%	11.19%

From the above table, it can be seen that if change in total shaft power prediction is compared with the change in experimental shaft power, it matches very well. So as mentioned above, it is possible that due to lack of experimental validation of gear, bearing and seal power loss the Table 2 and Table 4 comparison is not really indicating the correctness of the drag loss prediction model. Hence, the comparison presented in Table 5 can be referred as suitable experimental validation of the drag loss prediction model.

6. Accuracy and Uncertainty Analysis

The accuracy of the speed, pressure and, temperature sensors used during the experimental measurement is presented in the following table.

Table 6: Accuracy of instruments

Parameter	**Instrument**	**Specifications**
Compressor Speed, (N)	Digital tachometer, NCTM-1000, Metravi	Test Range: 2 to 99,9999 rpm Accuracy: ±0.05% ±1 digit
Temperature, (t)	RTD Pt-100, SIMPLEX Tempsens Instruments (I) Pvt. Ltd.	3-wire, DIN-43760, Class A Temperature range: -30°C to 350°C Accuracy: ±0.15°C at 0°C
Pressure, (p)	Pressure transmitter, MBS3000-2211-1 Danfoss	2-wire, 4-20 mA Pressure range: 0 to 16 bar, Accuracy:±0.5% FSD

During the experimental measurements, different sets of readings were recorded for the same operating condition. For ‘N’, ‘Beta-1’ and ‘Beta-2’, three, five and four sets of readings were recorded, respectively. An uncertainty analysis for each instrument reading is carried to understand the expected variation in the measurements (EDUCBA, 2022).

From the uncertainty analysis it is observed that the uncertainty in the pressure measurement is up to 0.03%, in the temperature measurement is up to 0.27%, in the manometer reading is up to 0.54% and in the speed measurement is up to 0.08%. The resultant effect on the suction volume flow rate variation when calculated is up to ±0.36%. An energy metre with a current transformer (225/5A) of 0.2 class accuracy was used for the measurement of the total compressor package power. The accuracy of the power measurement was ± 0.35% (Electrical Volt, 2022). The comparison results presented for shaft power in Table 5 are well outside the measurement uncertainty for the shaft power.

7. Conclusions

An analytical model for the prediction of drag loss in twin-screw, oil-flooded screw compressors is presented in the previous paper of this series while experimental validation of the same model using different screw rotor profiles is presented in this paper. A Kirloskar make 55 kW oil-flooded, twin-screw, air compressor was used for testing three different screw rotor profiles. These rotor profiles were assembled in the same housing, one after the other, and the compressor was operated under the same operating conditions followed by the measurements of suction volume flow rate and the shaft power.

The prediction of the shaft power for 'Beta-1' profile from the developed drag loss model matches closely with the experimental measurements. However, a slight deviation of ~1.3% in ‘Beta-2’ result was observed. During a detailed investigation of this deviation, it was found that highly negative gate rotor characteristics of ‘Beta-2’ rotors could have led to the rattling of the rotors (Stosic, 2017). This was confirmed by higher noise levels during testing as well as the metal-to-metal contact of the rotors observed after the disassembly of the compressor. These could be the reasons for the slightly higher experimental shaft power measurement in ‘Beta-2’ as compared to the prediction.

From the experimental measurements and their comparison with predictions, the proposed drag loss model is successfully validated and can be reliably used for different screw rotor profile configurations.

Acknowledgements

We gratefully thank Kirloskar Pneumatic Company Limited, Pune, India for sponsorship and Prof. Stosic, Prof. Kovacevic and Prof. Smith of City, University of London for their continued support and guidance.

Declaration of conflicting interests

The author(s) declared no potential conflicts of interest with respect to the research, authorship, and/or publication of this article.

Funding

The author(s) received financial support from Kirloskar Pneumatic Company Limited, Pune, India for the research and/or publication of this article.

References

1. Abdan, S., Stosic, N., Kovacevic, A., Smith, I., and Asati, N. Oil Drag Loss in Oil-Flooded, Twin-Screw Compressors. In *Journal of Process Mechanical Engineering*, accepted in June 2022 (under publishing)
2. Abdan S, Stosic N, Kovacevic A, Smith I, Deore P. Identification and Analysis of Screw Compressor Mechanical Losses. In *IOP Conference Series: Materials Science and Engineering*, 2018 Sep 1, Vol. 425, No. 1, p. 012015, IOP Publishing.
3. The SKF model for calculating the frictional moment, https://www.skf.com/in/products/rolling-bearings/principles-of-rolling-bearing-selection/bearing-selection-process/operating-temperature-and-speed/bearing-friction-power-loss-and-starting-torque (accessed December 2018).
4. Harris T, Kotzalas M. *Advanced Concepts of Bearing Technology: Rolling Bearing Analysis*, CRC press, 2006, chapter 10.
5. Tu M. *Validation and Modeling of Power Losses of NJ406 Cylindrical Roller Bearings*, MS Thesis, KTH Industrial Engineering and Management, Machine Design, Stockholm, Sweden, 2016.
6. Gradu M. Tapered Roller Bearings with Improved Efficiency and High Power Density for Automotive Transmissions. *SAE transactions*, 2000 Jan 1, 1696-705.
7. Deipenwisch R, Kauder K. Oil as a Design Parameter in Screw Type Compressors: Oil Distribution and Power Losses Caused by Oil in the Working Chamber of a Screw-type Compressor. In *IMECHE Conference Transactions*, 1999, Vol. 6. Mechanical Engineering Publications.
8. Gräßer, M., Brümmer, A. An Analytical Model of the Incompressible One-phase Clearance Flow in Liquid Injected Screw Expanders. In *9th International Conference on Screw Machines,* VDI Bericht 2228, 2014, pp. 71-89.
9. Gräßer, M., Brümmer, A. Influence of Liquid in Clearances on the Operational Behavior of Twin Screw Expanders. In *9th International Conference on Compressors and their Systems*, *IOP Conf. Series: Materials Science and Engineering 90*, 2015, 012060.

10. Gräßer, M., Brümmer, A. Influence of Water and Oil Clearance Flow on the Operational Behavior of Screw Expanders. In *Journal of Process Mechanical Engineering*, 2016. DOI:10.1177/0954408916667411.

11. Vasuthevan H, Brümmer A. Multiphase-flow Simulation of a Rotating Rectangular Profile within a Cylinder in terms of Hydraulic Loss Mechanisms. In *IOP Conference Series: Materials Science and Engineering*, 2018 Sep 1, Vol. 425, No. 1, p. 012002, IOP Publishing.

12. The Electrical Volt website for understanding of the current transformer measurement inaccuracy. https://www.electricalvolt.com/2020/10/what-is-the-difference-between-0-2-and-0-2s-class-ct/#:~:text=A%200.2S%20CT%20has,be%20guaranteed%20from%205%25%20loading (accessed June 2022).

13. HANJALIC, K., and N. STOSIC. "Development and optimization of screw machines with a simulation model-Part II: Thermodynamic performance simulation and design optimization." *Journal of fluids engineering* 119.3 (1997): 664-670.

14. Stosic, N. R. (1997). "Plural screw positive displacement machines", U.S. Patent No. 6,296,461. Washington, DC: U.S. Patent and Trademark Office.

15. Stosic, N. R. (2017). "Reduced noise screw machines", U.S. Patent No. 9,714,572. Washington, DC: U.S. Patent and Trademark Office.

16. Abdan S, Stosic N, Kovacevic A, Smith I, Asati N. Estimation of Radial Shaft Seal, Oil Drag and Windage Loss in Twin Screw Oil Injected Compressor. In *IOP Conference Series: Materials Science and Engineering 2021 Sep 1*, Vol. 1180, No. 1, p.012010, IOP Publishing.

17. Stosic, N. (2005). SCORPATH-Screw Compressor Optimal Rotor Profiles and Thermodynamics. http://www.staff.city.ac.uk/~ra600/DISCO/DISCO%20SCORPATH.htm (accessed December 2022).

18. EDUCBA, Uncertainty Formula. https://www.educba.com/uncertainty-formula/ (accessed December 2022).